Barotropic waves generated by storms moving rapidly over shallow water

Doug Mercer[1], Jinyu Sheng[2], Richard J. Greatbatch[2], and Joško Bobanović[2]

[1]Newfoundland Weather Centre, Environment Canada, Gander, NF,
Canada, A1V 1W7

[2]Department of Oceanography, Dalhousie University, Halifax, NS, Canada, B3H 4J1

Received ____________________; accepted ____________________

Short title: BAROTROPIC WAVES GENERATED BY RAPIDLY MOVING STORMS

SUBMITTED TO **JGR-OCEANS ON SEPTEMBER 7, 2001**

Abstract.

In the fall of both 1999 and 2000, waves with characteristics similar to tsunami hit the southeast coast of Newfoundland, Canada. The waves were large enough to cause local flooding, damage to docks, and other destruction. There is, however, no evidence of seismic events, underwater landslides or slumping events on either occasion. Other explanations, such as storm surge, also appear unlikely, and local weather conditions at the coast were not exceptional at the time.

On both occasions, tropical storms moved rapidly across the Grand Banks of Newfoundland from southwest to northeast, with a translation speed of ≈ 30 ms^{-1}. A significant, non-isostatic response to atmospheric pressure forcing can be expected over the shallow water of the Banks, since the translation speed of the storms is comparable to the local shallow water gravity wave speed. We speculate that the atmospheric pressure forcing associated with the storms generated a barotropic wake, and use a numerical model to argue that as the storm moved back over the deep ocean, the wake was refracted and/or reflected by the variable bathymetry at the edge of the Banks, and that it was the refraction of the wake towards the coast that led to the unusual sea level events in southeastern Newfoundland.

The numerical model results are in general agreement with the eye-witness reports. The model-computed wave activity hits the southeast coast of Newfoundland at about the right time and in the right areas for both events, although for the 1999 event the model response is weaker than observed at Port Rexton in Trinity Bay. The reason for the poorer model performance in the 1999 case is not known, although we do find that the model results are sensitive to uncertainty in the exact track taken by the storm across the Banks. The model results demonstrate that the period and wavelength of the gravity waves comprising the wake are, in general, proportional to the length scale of the pressure forcing, an exception being the model response in Conception Bay, Newfoundland, where a resonant seiche response is found to dominate.

1. Introduction

Near dusk on October 25, 1999, the Newfoundland Weather Centre received a telephone call describing an unusually rapid "tide" at Port Rexton in Trinity Bay (Figure 1). The water in the port was rising and falling with a period of tens of minutes and peak-to-trough displacement of 2 to 3 m, destroying the local wharf. Over the next few days other reports of the same event came in from Trinity Bay and other coastal areas along the east coast of the Avalon Peninsula, giving generally similar accounts of the wave behaviour. Near the same time, an Acoustic Doppler Current Profiler deployed in St. John's Harbour detected an unusually strong current flowing in and out of the harbour mouth with a period of tens of minutes (de Young et al., 2000). Note that near the time of onset of the event, the tide was near a spring high tide, and the weather conditions over the coastal areas were generally good with light to moderate northwesterly winds and very little surface wave action in the harbours in question.

The wave behavior at the various harbours is generally consistent with barotropic shallow water gravity waves (Gill, 1982). The total event lasted for about one to three hours, with a wave period of tens of minutes. The wavelength is long enough so that most witnesses reported just rises and falls of the water level, although some long, narrow, and shallow harbours reported a tidal bore. Most harbours affected were facing approximately eastward. These characteristics are consistent with tsunami-like waves generated and propagating from the east.

Upon checking with the Geological Survey of Canada, there were no seismic events in either Eastern Canada or the Atlantic Ocean of sufficient magnitude to produce a tsunami within the previous 24 hours (Wetmiller, Geological Survey of Canada, personal communication). The next most likely cause is a sufficiently strong underwater landslide or slumping event. While these events are admittedly harder to detect seismically, there is no evidence for their occurrence. Also, there is little silt near the shelf break on the eastern or southeastern edges of the Grand Banks to initiate a significant slumping event. Note that it would be necessary for something with a length scale of tens of kilometres to force a barotropic wave with the observed period. This is because the shallow water gravity wave speed over most of the Grand Banks is about 30 ms^{-1}. Therefore, a shallow water gravity wave with a period of 30 minutes should have a wavelength of about 54 km on the Banks.

On that day of October 25, 1999, Tropical Storm Jose approached the Grand Banks from the southwest with a translational speed of $\approx$ 32 ms^{-1} or 60 knots (Figure 2). It passed east of the Banks at about 15:30 local time and the coastal effects occurred about 3 to 4 hours later. This raises the possibility that the unusual events observed at the coast can be explained by waves generated in the vicinity of the storm and propagating towards the shore. If the wave propagates from the eastern shelf break of the Grand Banks at the average shallow water wave speed for this area ($\approx$ 30 ms^{-1}), it would reach the shore at about the right time. Note also that the translation speed of the storm was near the local gravity wave speed over the Grand Banks ($\approx$ 30 ms^{-1}), suggesting a significant non-isostatic ocean response to the atmospheric pressure forcing by the storm (see Section 2), which we believe generated the waves in question.

On a beautiful fall afternoon on September 25, 2000, similar reports started coming in (Figure 1). As before, over the coastal region little wave action prevailed with generally light winds. Areas along the east coast of the Avalon Peninsula which reported events in 1999 had almost identical descriptions of the events in 2000, with the intensity being a little higher in 2000. The main difference between 1999 and 2000 lay in the areas affected. There were no unusual reports in Trinity Bay (as opposed to two in 1999), while many communities along the southern half of Conception Bay consistently reported rises and falls of sea level of about 2 m (while there were no reports in 1999). Also, Conception Bay was affected about an hour after the east coast. Again, there is no evidence of a significant seismic event (Drysdale, Geological Survey of Canada, personal communication).

On that day, Tropical Storm Helene traveled across the Grand Banks on a similar path to Jose of the previous year, but closer to the Island of Newfoundland (Figure 2).

Again, it was a compact storm moving over the Grand Banks with an average speed of ≈ 32 ms^{-1} (60 knots). It is interesting to note that, as in the previous year, the coastal events occurred several hours after the storm crossed the Banks. The fact this happened on both occasions supports the view the coastal events were a consequence of the offshore storms.

There has been little or no study of the generation of (non-rotating) barotropic shallow water gravity waves by storms traveling over the Grand Banks of Newfoundland. Furthermore, to our knowledge this type of event has not previously been reported in Newfoundland. Nevertheless, there is evidence that translating atmospheric disturbances can generate barotropic gravity waves with significant consequences. Ewing et al. (1954), Donn (1959) and Abraham (1961) discuss unusually large and rapid changes in water level around the shores of the Lake Michigan and Lake Erie, which they attribute to translating atmospheric disturbances. In each case, the disturbance was translating at a speed comparable to the local shallow water gravity wave speed in the lake, implying a significant non-isostatic response to the atmospheric pressure forcing. In the case of the event in Lake Michigan in 1954, Ewing et al. (1954) also suggest that refraction and reflection of the waves by the variable water depth played a role, something we believe is important for explaining the events associated with Tropical Storms Jose and Helene (see Sections 2 and 3). Ewing et al.'s conclusions were largely verified by Platzman (1956, 1965), leading to the setting up by the US Weather Bureau of an operational warning system in Lake Michigan (Irish, 1965; Hughes, 1965; Churchill et al., 1995). Similar phenomena have been reported along the Atlantic coast of the US. Harris (1956) and Abraham (1961) have noted that Hurricane Carol (1954) traveled northwards over the mid-Atlantic Bight at a speed comparable to the local gravity wave speed and suggest that part of the storm surge associated with Hurricane Carol (1954) was associated with barotropic gravity waves generated by the atmospheric pressure forcing associated with the storm. Also, a large wave at Daytona Beach in July 1992 is discussed by Churchill et al. (1995) who attribute the wave to forcing by an offshore squall line.

In this paper, we describe and numerically demonstrate a mechanism by which storms, such as Tropical Storms Jose and Helene, can generate barotropic gravity waves as they move across the Grand Banks of Newfoundland, these waves in turn impinging on the coast and leading to a significant nearshore response, consistent with the eye-witness reports. The large, flat, and shallow region of the Grand Banks means that very rapidly moving storms can be translating at close to the local shallow water gravity wave speed (as in the cases of Jose and Helene), and, depending on the storm track, to do this for long distances. This leads to a strong non-isostatic response to the atmospheric pressure forcing associated with the storms, and the generation of a barotropic wake. We show how the wake is refracted by the variable bottom topography and reflected back from the shelf break toward southeastern Newfoundland, and how this explains most of the spatial distribution and the timing of the observed events. In Sections 2 and 3, we describe and illustrate the basic theory as applied to our problem, and provide a brief description of the numerical model. Section 4 presents the model results using realistic bathymetry and forcing, including a discussion of the sensitivity of the model results to the size and intensity of the storms producing the waves, and to the track taken by the storms over the Grand Banks. Finally, Section 5 provides a summary and conclusions.

2. The basic theory and the numerical model

The focus of this paper is barotropic gravity waves with periods of tens of minutes, which implies, over most of our domain, wavelengths of tens of kilometres, forced by a highly localized storm with a core of similar dimensions. The governing equations are the vertically integrated shallow water equations for a homogeneous fluid with a free surface, allowing both atmospheric pressure and wind stress forcing. The grid is Cartesian with positive x, y and z being east, north, and up, respectively, with $z = 0$ at mean sea level. The perturbation pressure p' is given by

$$p' = p'_a + \rho g \eta \tag{1}$$

where p'_a is the perturbed atmospheric pressure, g is the gravitational constant, and η is the upwards displacement of the free surface. Water density ρ is assumed uniform and constant. Equation (1) may be rewritten

$$p' = \rho g \eta' \tag{2}$$

where $\eta' = \eta - \eta_a$ is the adjusted sea level. η_a is the change in surface elevation of an inverse barometer (Gill, 1982) and is given by $\eta_a = -p'_a/\rho g$. (Note that strictly speaking, the inverse barometer includes a contribution from the global average of the surface pressure that arises from the assumption that the ocean is an incompressible fluid. This contribution is not important for our discussion and so, for simplicity, is ignored.) The forced shallow water equations are then

$$\begin{aligned} \frac{\partial u}{\partial t} - fv &= -g\frac{\partial \eta'}{\partial x} + \frac{\tau^x}{\rho H} - \frac{ru}{H}, && (3) \\ \frac{\partial v}{\partial t} + fu &= -g\frac{\partial \eta'}{\partial y} + \frac{\tau^y}{\rho H} - \frac{rv}{H}, && (4) \\ \frac{\partial \eta'}{\partial t} + \frac{\partial (Hu)}{\partial x} + \frac{\partial (Hv)}{\partial y} &= -\frac{\partial \eta_a}{\partial t} && (5) \end{aligned}$$

where (u, v) are the eastward and northward velocity components, respectively, (τ^x, τ^y) are the surface wind stress components, f is the Coriolis parameter, r is a linear bottom friction coefficient, and H is the local water depth.

2.1 Basic theory

The time scales of interest (several hours at most) are such that we can neglect the effects of the Coriolis parameter and bottom friction in the following discussion. The numerical results to be presented in Section 3 do include the Coriolis term and bottom friction, but putting these terms to zero has only a small effect on the model results. We also find that the effect of atmospheric pressure forcing dominates that of wind forcing, so it is appropriate to consider atmospheric pressure forcing only. It is then easy to show that the equation governing the adjusted sea level, η', is

$$\eta'_{tt} - (c^2\eta'_x)_x - (c^2\eta'_y)_y = -\eta_{att}, \tag{6}$$

where $c = \sqrt{gH}$ is the local gravity wave speed. For a flat-bottomed ocean, this reduces to

$$\eta'_{tt} - c^2(\eta'_{xx} + \eta'_{yy}) = -\eta_{att}. \tag{7}$$

For the case of a flat-bottomed ocean, it is convenient to consider a steady storm that is translating at a uniform speed $U > 0$ along the x-axis in the direction of positive x, and seek solutions that are translating steadily with the storm. We therefore follow Geisler (1970) and Greatbatch (1983) and define a new coordinate $\xi = x - Ut$. From Eq. (7), it then follows that steady, translating solutions for η' satisfy

$$(U^2 - c^2)\eta'_{\xi\xi} - c^2\eta'_{yy} = -U^2\eta_{a\xi\xi}. \tag{8}$$

It is immediately apparent that the character of the governing equation is elliptic if $U < c$, but is hyperbolic if $U > c$ (Geisler, 1970). It follows that in the latter case, the storm generates a wake, analogous to the wake generated by a ship, that propagates out from the storm track behind the storm. As we shall see, the wake is most efficiently generated when $U \approx c$. It should be noted, however, that there is no singularity when $U = c$, and that the transition from elliptic to hyperbolic behavior is a smooth one. Indeed, the two-dimensional problem we are considering here differs from its one-dimensional equivalent, in that there is no resonance when $U = c$, because energy is free to propagate away from the storm track. It should also be noted that when $U \ll c$, as is typically the case in the deep ocean, the response to the storm will be isostatic, with $\eta' \approx 0$.

Figure 2 shows a plot of the local gravity wave speed $c = \sqrt{gH}$. The mean water depth on the Grand Banks is around 80 m for which the mean gravity wave speed is ≈ 30 ms^{-1}, but is as low as 20 ms^{-1} in some places. This is very close to, or slightly less than, the propagation speed of both Jose and Helene. Over the Banks, therefore, we expect a strongly non-isostatic response to the atmospheric pressure forcing associated with these storms, including the possibility of a barotropic wake. On the other hand, in the deep water beyond the shelf break, where the water depth is typically 4000 m and the wave speed is ≈ 200 ms^{-1}, we expect an almost isostatic response with $\eta' \approx 0$. The sharp contrast between the gravity wave speeds of several 10's ms^{-1} on the Banks, compared to several 100's ms^{-1} beyond the shelf break, raises the possibility of interesting refraction behavior as the waves generated by the storm propagate over the Banks and interact with the shelf break. As we shall see in the model results to follow, the gravity wave wake generated by the storm can be refracted from the shelf break back towards the coast. Indeed, we believe this is what happened in the case of the events associated with Tropical Storms Jose and Helene, and that it was the energy refracted back towards the coast that led to unusual sea level events that were observed.

2.2 The numerical model and surface forcing

The numerical model used is a modified version of the storm surge model developed by Bobanović and Thompson (2001). It is linear and barotropic, and solves the governing equations (3)-(5) with variable bathymetry using the Arakawa C-grid for the horizontal grid arrangement. The model is forced by atmospheric pressure. Experiments including wind forcing, using the formulation of Large and Pond (1981) to convert wind velocity to surface wind stress, show that the effect of wind forcing is negligible compared to that of pressure forcing at the coast, and so will be ignored. The linear bottom friction coefficient r used in the numerical experiments has value 0.001 ms^{-1} unless otherwise stated, but it can be set to zero without significantly affecting the model results. Outgoing waves at open boundaries are handled by a radiation condition (Chapman, 1985).

Unfortunately, we do not have sufficient information from observations or operational analyses to specify the precise structure and magnitude of the surface forcing associated with the tropical storms. We therefore use an idealized form for the surface forcing in the numerical experiments. In particular, the atmospheric pressure field is specified as

$$p_a(x, y, t) = p_o - \Delta p \; exp\left[-\frac{(x - x_s(t))^2 + (y - y_s(t))^2}{\sigma^2}\right], \tag{9}$$

where p_o is the mean sea level pressure and set to 101 kPa in this paper, Δp is the maximum pressure drop associated with the storm, $(x_s(t), y_s(t))$ are the coordinates for the center of the storm, and σ is defined at the "radius" of the storm. Since there are no direct measurements of the storm central pressures and sizes for either storm (Newfoundland Weather Centre, personal communication), we set Δp to be 3 kPa, giving the best estimate of the pressure drop for the two storms. We also set σ to 40 km, giving an effective "eye-wall" radius of about 30 km. The sensitivity to the specification of σ is discussed in Section 4.3.

3. Numerical simulations using idealized bathymetries

In order to illustrate the model behaviour, we first use a rectangular ocean basin with idealized bathymetry on an f-plane centered at 45°N. The dimension of the domain is 1500 km in the eastward and 500 km in the northward direction, respectively. A model grid spacing of 3 km and time step of 20 s is used so that we can easily resolve horizontal length scales of tens of kilometers and time scales of tens of minutes. The initial condition is a state of rest with a uniform surface pressure of 101 kPa and a flat ocean surface. In all runs presented in this section, the pressure forcing defined in Eq. (9) is switched on impulsively at the beginning of integration, with the initial position of the storm center located at the western boundary and halfway between the northern and southern boundaries (i.e. $x_s(0) = 0$ and $y_s(0) = 250$ km). For $t > 0$, the low pressure system is moved eastward at a constant speed U of about 31 ms^{-1} (U approximates the translation speeds of Jose and Helene across the Grand Banks and was chosen to be equal to the barotropic shallow water wave speed for a depth of 100 m). The wind forcing is set to zero throughout.

We begin by considering a storm moving over a flat-bottomed ocean with water depths of 156m, 100m, and 25m, respectively, and for which $U/c = 0.8$, 1.0, and 2.0. Figures 3a,c,e show the adjusted surface elevation, η', 10 hours into the model run, at which time the system is in quasi-equilibrium. Figures 3b,d,f show time series of the adjusted sea level at the locations A and B in Figures 3a,c,e. When $U/c = 0.8$, there is a setup of the adjusted sea level in the near field of the pressure forcing (Figure 3a). The setup is roughly symmetric with respect to the center of the storm and moves eastward with the storm. The maximum setup at 10 hours is about 20 cm. Note that weak disturbances ahead of the system propagate eastward at the shallow water gravity wave speed, which, in this case, is 25% faster than the translation speed of the storm.

By contrast, a large wake is generated when $U/c = 1$ (Figures 3c and d). The wake consists of a large setup or rise centered slightly behind the storm center and led by a setdown of similar size. The maximum setup and setdown at 10 hours are about 110 cm and 70 cm, respectively. Note that in the near field of the storm, the model response is a combination of waves being generated near the time of the snapshot and waves generated at an earlier time and which propagate in the same direction as the storm. In the far field, on the other hand, the wake consists only of waves generated earlier and which have propagated outward from the storm track. Figure 3d also shows that the wave at site B lags slightly behind that at site A, indicating that the angle between the wake and the storm track is not quite 90°. The steady-state solution for Eq. (8) implies that (neglecting bottom friction), the wake in the steady-state should be perpendicular to the storm track in the case $U/c = 1$. This ideal shape is due to the integrated contribution from forward propagating waves generated over an infinitely long storm track history. As time goes by, and energy from further back along the storm track contributes to the wake, so that the angle between the wake and the storm track becomes closer to 90°, as can be verified with the model.

Figures 3e and f show that a large wake is also generated by the pressure forcing when $U/c = 2$, although its magnitude is much smaller than that in the case of $U/c = 1$. The wake again consists of a setup and setdown. The maximum setup and setdown in this case are about 25 cm and 30 cm, respectively. Since the storm moves much quicker than the gravity waves, the waves generated at earlier times trail behind the storm in a V shape, as we expect given the hyperbolic nature of the governing equations (Eq. (8)). Theoretically, the angle between the wake and the storm track (α) is given by $\alpha = \arcsin(c/U)$ if effects in the storm near-field and bottom friction are neglected. In the case of $U/c = 2$, the angle is 30°, in agreement with the theory.

To examine the sensitivity of the model results to the value of U/c, we carried out ten additional runs using a flat-bottomed ocean with water depths ranging from 25 m to 625 m. The mean features of these runs are qualitatively similar to Figure 3a for $U/c < 1$, and to Figure 3c for $U/c > 1$, but with strong dependence of the wave amplitude on U/c. Figure 4 presents the maximum setup (η'_{max}) and maximum setdown ($|\eta'_{min}|$) determined from time series at site A for all thirteen runs. Both η'_{max} and $|\eta'_{min}|$ are near zero for $U/c < 0.5$, indicating a nearly isostatic response if the storm speed is slower than the half of the gravity wave speed. These values increase sharply, however, for $0.8 < U/c < 1$ and reach maxima at $U/c \approx 1$, indicating that a wake is generated most efficiently by the pressure forcing when the storm speed is equal to the gravity wave speed. Finally, η'_{max} decreases significantly with U/c for $1 < U/c < 1.2$ and more gradually for $U/c > 1.2$. $|\eta'_{min}|$, on the other hand, approaches 30 cm as U/c increases, which just means that the total sea level $\eta = \eta' + \eta_a$ does not change much due to the rapid transit of the pressure system over the water (η' mostly cancels the inverse barometer effect η_a which has magnitude 30 cm).

We next investigate the impact of including a shelf break. We expect that the variable local gravity wave speed, $\sqrt{gH}$, associated with the variable bathymetry, leads to significant wave refraction, and possibly reflection. To answer this issue, we describe two numerical experiments that use model bathymetry consisting of water of uniform depth 75 m and 400m in the western and eastern part of the model domain, respectively, the two flat regions being connected by a shelf break. In the first experiment, the shelf break is abrupt, with the water depth changing from 75 m to 400 m over one grid box (Figure 5a). In the second experiment, the shelf break is much wider with the water depth increasing linearly from 75 m to 400 m over 120 km distance (Figure 5b). The pressure forcing is again Eq. (9), with its initial position at the centre of the western boundary. The pressure field is moved eastward at a constant speed of 31 ms^{-1}. As a result, U/c is 1.15 and 0.5 for the western and eastern parts of the domain, respectively.

Figure 5 shows snapshots of the adjusted sea level in the two experiments. Before the storm reaches the shelf break, the main features of the adjusted sea level are qualitatively similar to Figure 3e. Upon interacting with the shelf break, a significant part of the wave energy is reflected back from the shelf break, and at 5 hours, is seen to be propagating in the opposite direction to the storm. The details of the reflection process are different in the two cases. When there is a gradual slope (Figs.5b,d,f), the waves are seen to propagate on to the slope and then be refracted back up the slope by the increased wave propagation speed in deeper water. When there is an abrupt change in depth, the reflection happens much more quickly so that the reflected waves influence upstream locations sooner than in the gradual sloping case (cf. Figs.5e,f). As we shall in the next section, our realistic simulations also show refraction and reflection of waves by the variable bathymetry at the shelf break.

4. Numerical simulations using realistic bathymetry and storm tracks

We now use the numerical model to study the generation of shallow water gravity waves over the Grand Banks in association with Tropical Storms Jose and Helene. The model domain covers the area between 41°N and 50°N and between 56°W and 43°W (Figure 2), with realistic bathymetry except that water depths greater than 1000m are set to 1000m. Since for 1000m depth, the ratio $U/c \approx 0.3$, for which the model response is close to isostatic (see Figure 4), the use of a 1000m cut-off has no significant impact on the model results. The model resolution is 1/24th of a degree in both the eastward and northward directions and the time step is 20 s. The atmospheric pressure forcing takes the same form as given by Eq. (9) with σ set to 40 km. The storm moves along the observed storm tracks, and forcing by the surface wind stress is not included since this was found not to be important for the model response.

4.1. Tropical Storm Helene (September, 2000)

Tropical Storm Helene developed from a tropical wave that emerged from the African coast on September 10, 2000. It moved northwestward through the Caribbean Sea and then through the Gulf of Mexico to hit the southeastern United States on the 22nd and 23rd and then turned northeastward to enter the North Atlantic Ocean on the 24th. Helene approached the study region from the southwest on the 25th with an average translational speed of about 30 ms^{-1}. It moved on to the Grand Banks at about 1400Z (Zulu or equivalently Universal Coordinated Time, UTC) and back into the deep ocean to the east of the Banks at about 1900Z (Figure 2).

We integrate the numerical model for 24 hours, starting from 0600Z on the 25th. The center of the storm at that time was located at 62.2°W and 41.6°N, which was about 450 km away from the model western boundary (Figure 2). Figure 6 shows snapshots of the model-calculated adjusted sea level (η') as the storm crosses the Grand Banks. Adjusted sea level due to the pressure forcing is negligible over deep water before the storm reaches the Grand Banks, consistent with the model results for $U/c << 1$ shown in Section 3. Once the storm moves on to the Grand Banks at about 1400Z, a wake is immediately generated (Figure 6a), the wake spreading outward from the storm track as the storm moves northeastward. The wake consists of a setdown ahead of the storm center and a setup of similar size behind the center, as seen in Section 3. The maximum setup and maximum setdown at 1630Z are about 60 cm and 40 cm, respectively (Figure 6c).

As the storm approaches the eastern edge of the Grand Banks near 1800Z, the storm-generated waves to the right of the storm track reflect back on to the Banks (Figures 6c). By 1930Z the storm is over the western flank of Flemish Cap, and the wake is now left behind over the Grand Banks (Figure 6d). Note that there are no large waves generated in the near field of the storm at this time, due to the almost isostatic response to the pressure forcing in deep water. Meanwhile, the waves generated earlier to the left of the storm track are now refracted around the eastern edge of the Grand Banks (Figures 6c and d), leading to shoreward propagation of the barotropic gravity waves along the northern edge of the Banks (Figure 6e). These waves undergo significant refraction due to the curvature of the bathymetry contours around the northern edge of the Banks (Figures 6c to e). By 2200Z the gravity waves impact the coastal areas, leading to a significant sea level response in southern Conception Bay and along the east coast between St. John's and Cape Race (Figure 6f and Figure 1).

Figure 7 shows time series of adjusted sea levels at five coastal stations along the Avalon Peninsula. In the model, the main wave train reaches Bay Bulls and St. John's at about 2130Z. This is consistent with the witness reports from the two harbours. Figure 7 also shows the main wave train arriving at Holyrood about a half hour later than at Bay Bulls and St. John's, which again is consistent with the witness reports. Given the uncertainty in the magnitude of the pressure forcing associated with the storms, and the possibility of local amplification of the response in shallow water near the coast, the amplitude of the model-computed response is broadly consistent with the witness reports, and does show a range in sea level of up to 2 m at Holyrood, similar to what was reported from Conception Bay.

Let us now examine the model behaviour in more detail. Figure 8 shows close-up plots of the adjusted sea level and the model-computed currents around the Avalon Peninsula. The relationship between currents and sea level are characteristic of non-rotating gravity waves, as we expect, with sea level rise (fall) being generated in regions of convergence (divergence) of the two-dimensional flow. For example, Figure 8a indicates onshore flow between Bay Bulls and Port Rexton at 2130Z, resulting in a rise in sea level along the coast. The adjusted sea levels reach a peak of about 10 cm around 2130Z at Port Rexton, 10 cm around 2140Z at St. John's, and 30 cm and 40 cm around 2150Z at Bay Bulls and Holyrood, respectively (Figure 7).

A half hour later at 2200Z, the model-calculated depth-mean flows are roughly offshore over the coastal areas from Bay Bulls to Port Rexton (Figure 8b), with the strongest outflows in Conception Bay. This leads to significant drops in sea level over these areas (Figures 7a-d). The adjusted sea levels reach a maximum setdown of about 20 cm around 2200Z at Port Rexton, 40 cm around 2210Z at St. John's, 50 cm around 2220Z at Bay Bulls, and 80 cm around 2230Z at Holyrood (Figure 7). In contrast, the depth-mean currents are weak over the coastal areas off the west coast of the Avalon Peninsula with negligible sea surface elevations at Argentia during this period (Figure 7e).

Figures 8c and d reveal that the depth mean currents inside Conception Bay change from weak outflows at 2230Z to strong inflows at 2300Z. The currents in Trinity Bay also change from outflows to inflows during this period, but with much smaller magnitudes. As a result, the coastal sea levels rise to reach a maximum setup of about 20 cm around 2230Z at St. John's, 40 cm around 2300Z at Bay Bulls, and 100 cm around 2310Z at Holyrood (Figures 7a-c). In contrast, the adjusted sea levels at Port Rexton are small and actually decrease during this period (Figure 7d). Over the coastal areas off the west coast of Avalon Peninsula, around Argentia, the depth mean flows and adjusted sea levels remain weak.

Figure 9 shows the maximum setup at each location. The greatest setup occurs in Conception Bay with a magnitude of greater than 100 cm at the head, where Holyrood is located. The maximum setup is about 30 cm in Trinity Bay and along the east coast from Cape Race to Bay Bulls. The maximum setup is relatively small over the south coast of the Avalon Peninsula, except for the head of the Placentia Bay, north of Argentia. It should be noted that there were no witness reports from the western side of the Avalon Peninsula, and there is no evidence of unusual wave activity from the tide gauge at Argentia. While not conclusive, this is consistent with the weak signal shown in this region by the model (Figures 6 and 9).

Note that there are some differences between the model simulation and witness reports. The major discrepancy is the period of the sea level excursions characterizing the event at the coast. On the east coast of the Avalon Peninsula, the witness reports generally give a period of about 10 to 30 minutes, while the model simulation gives a period of about 60 minutes. One possible reason is local seiching, e.g. within individual harbours, that is not resolved by the numerical model (we use a resolution of 3 km). The fact, however, that the discrepancy is found everywhere suggests that a more likely reason is the choice of the length scale σ for the storm size used in the simulation (see Eq. (9)). The results of the sensitivity studies to be presented in Section 4.3 support this view.

4.2 Tropical Storm Jose (October, 1999)

Tropical Storm Jose originated from a tropical wave that moved off the west coast of Africa on October 8, 1999. Jose first moved slowly westward across the tropical Atlantic Ocean for several days, then turned northward and subsequently north-northeastward on the 22nd. Jose approached the Grand Banks from the southwest on the 25th with an average translational speed of about 30 ms^{-1}. The storm moved onto the Grand Banks around 1400Z on the 25th and moved back into the deep waters at about 1530Z (Figure 2). Therefore, Jose was over the Grand Banks for only one and a half hours, which is much shorter than Tropical Storm Helene (about five hours).

As before, we integrate the model for 24 hours, starting from 0600Z on October 25, 1999. The center of the storm at this time was located at 55.8°W and 37.9°N, about 400 km from the southern model boundary. Figure 10 shows snapshots of the resulting adjusted sea levels. As before, there are no significant gravity waves generated by the storm over the deep water before the storm reaches the Grand Banks. Once the storm reaches the Grand Banks (1400Z), a wake with a setup and setdown of similar size is immediately generated in the near field of the pressure forcing (Figure 10a), which is very similar to the onset of the wake generated by the Tropical Storm Helene (Figure 6a). In contrast to Helene, the wake generated by Jose has less time to develop before the storm crosses the eastern shelf break and moves back over deep water around 1600Z. At this time, the influence of the variable bottom topography on the waves generated over the Banks is already apparent (Fig 10b). By 1730Z, the gravity waves associated with the wake are propagating northwestward across the Grand Banks towards the coast (Figures 10c and d). By 2030Z, the waves are already impacting the east coast of the Avalon Peninsula.

Time series of the adjusted sea levels at the five coastal stations are shown in Figure 11 for the Jose case. A comparison of Figures 7 and 11 indicates that the impact of the remotely generated waves in the Jose case is very similar to that in the Helene case, but with smaller amplitude (Figures 7 and 11). A significant difference with the Helene case is the timing of onset at different stations. The main wave train impacts Bay Bulls and St. John's around 2000Z, and Holyrood and Port Rexton roughly one hour later. This is clearly due to the main wave propagating in from the southeast.

The adjusted sea levels at Bay Bulls and St. John's have similar temporal variability, with the main event lasting about two hours. At Holyrood and Port Rexton, the event is longer lasting. The adjusted sea level inside the main wave train rises gradually and then falls significantly to reach a maximum setdown, then rises again to reach a maximum setup. The maximum setdown is about 30 cm at Bay Bulls around 2020Z, 25 cm at St. John's around 2030Z and 25 cm at Holyrood around 2110Z. The adjusted sea level elevations are relatively small at Port Rexton and Argentia.

Figure 12 shows the the maximum setup computed by the model. The greatest setup occurs at the heads of Conception Bay, Trinity Bay and Trepassey Bay to the west of Cape Race. The maximum setup is about 10 to 20 cm over the east coast from Cape Race to St. John's, and negligible over the west coast of Avalon Peninsula.

The model-calculated wave characteristics roughly approximate the witness reports and data in the region. The ADCP data collected in St. John's harbour show high-frequency fluctuations in the measured flow that started around 2000Z and lasted for about one and half hours. This is consistent with the model results presented in Figure 11b. Similarly, the witness reports for the unusual waves at Port Rexton give the onset of the waves to be around 2115Z with errors of $\pm$ 0.75 hours, which is again roughly consistent with the model results shown in Figure 11d.

The most notable discrepancy between the model and the witness reports is the relatively small amplitude of the model response at Port Rexton. We think this may be related to uncertainty in the exact track followed by Jose over the Banks, an issue that is discussed further below.

4.3 Sensitivity Studies

Studies were performed to examine model sensitivity to standard parameters such as the grid size, the time step, the Coriolis effect, and bottom friction, none of which were found to have a significant impact on the model results. Of greater concern is the sensitivity to the specification of σ in Eq. (9) (i.e. storm size), and the storm track.

As noted earlier, the main discrepancy between the model results and the witness reports is in the period of the sea level excursions comprising the events which was typically observed to be between 10 and 30 minutes, compared to roughly 60 minutes in the model simulations. We believe the most likely reason for this is the choice of 40km for the length scale, σ, used in Eq. (9) to define the pressure forcing. Since we are considering non-rotating, shallow water gravity waves, we expect that halving this length scale will halve the wavelength of the excited waves, and, hence, half the period, bringing it more in line with the witness reports. It should be noted that the details of the storms were not well resolved either by the Canadian GEM regional model or by operational data analyses, so there is considerable uncertainty in the choice of length scale. To test the sensitivity to σ, model simulations for both the Helene and Jose cases were run using specifications for σ from 20 km to 160 km. For the Helene simulations, the strongest wakes were obtained for $\sigma = 20, 40$ and 80 km. We choose Bay Bulls (Figure 13a) as representative of the east coast and Holyrood (Figure 13b) as representative of Conception Bay. For larger length scales the period is far too long to match the observed events, and the wake energy is spread over too large an area. As expected, for Bay Bulls the length scale, and the period of the wake, increases with the length scale σ. The 20km case has a period after onset of close to half an hour, near 1 hour in the 40km case, and about 2 hours in the 80 km case. Results for Bay Bulls in the Jose simulations are qualitatively similar but weaker in amplitude (Figure 13c). Note that the time of onset of the event is relatively insensitive to σ, as we expect for the non-dispersive gravity waves being considered here.

The results for Holyrood (southern Conception Bay) show a different type of response (Figure 13b). For $\sigma = 20$ km, the response at Holyrood has a peak to trough amplitude of near 0.6 metres (comparable to but a little weaker than the Bay Bulls response). But for $\sigma = 40$ and 80 km, the peak to trough amplitude is near 1.8 metres and is somewhat bigger than at Bay Bulls. Also, the period is near 1.5 hours in all three cases (it does increase with σ, but only slightly). This is probably due to the fundamental seiching period of the bay. If we assume the bay is a quarter-wave oscillator of 60 km length and depth 200 m (both length scales are characteristic of Conception Bay), the seiche period is about 1.5 hours. The excitation of the seiche probably also explains why the strongest signal is the model is found in the 40 and 80 km cases, since in these cases, the dominant period outside Conception Bay is closest to the fundamental resonance period of the bay. Again, results for Holyrood in the Jose simulations are similar (Figure 13d).

Next we consider the sensitivity to small changes in the storm track. Figure 14a,b shows the result of varying the track of Helene by 0.5^o to the north and south. It is seen that the biggest impact is obtained by moving the storm track to the south. Of more interest is the impact of changing the track of Jose. From the data available (Figure 2), the storm barely clipped the southeastern corner of the Grand Banks, and would have been able to generate a barotropic wake for less than 90 minutes. But a small change in the trajectory to the left of the "official" track significantly increases the trajectory over shallow water.

We therefore perturbed the track of Jose 0.5^o and 1.0^o to the northwest. Figures 14c and d show the sea level at Bay Bulls and Holyrood due to the original track and the two perturbed tracks mentioned above. Moving the track half a degree northwest makes a small increase in the amplitude of the wave, and some small difference in the time of onset of the event. On the other hand, moving the storm track one degree to the northwest has a much bigger impact, leading to a stronger response at both Bay Bulls and Holyrood, and delay in the time of onset of the event, which now occurs simultaneously, and roughly in phase, at both locations. The change in the wave pattern is due to the perturbed storm track causing the storm centre to be over or near shallow water for a much longer trajectory, with the system moving off the Banks in a region that produced a refracted wave that moved back towards Newfoundland along the edge of the Banks, as in the Helene case. These results indicate the importance of correctly specifying the storm track.

In the case of Jose, the changes to the storm track considered here do not improve the model performance at Port Rexton where the amplitude of the model response is weak in comparison with the eye-witness reports. The reasons for the discrepancy are unknown at this time.

5. Summary and Discussion

In this paper we investigate unusual wave events observed in southeastern Newfoundland in the falls of 1999 and 2000. We believe these wave events to be associated with the passage of Tropical Storms Jose (1999) and Helene (2000) across the Grand Banks of Newfoundland. The shallow water depth on the Banks ($\approx$ 80 m) means that as the storms propagated across the Banks, their translation speed was comparable to the local shallow water gravity wave speed, implying a significant non-isostatic response to the atmosphere pressure forcing by the storms. We used a simple, linear, barotropic model with a free surface to verify this idea. We also found that the wakes produced by the storms are refracted and reflected by the variable bathymetry around the edge of the Banks, and we believe it was waves refracted in this way that impacted on the coast of Newfoundland. While the generation of such wakes have been observed and studied previously in the Great Lakes, there has been no scientific observation or previous study of the refraction/reflection of such waves over the Grand Banks of Newfoundland that we are aware of.

The model-computed wakes are found to be generally consistent with the witness reports. In particular, the events at the coast occurred at about the right times (usually well within an hour of the witness reports). The areas affected in 2000 match the model output very well. In 1999, the model correctly predicts a significant impact on the east coast of the Avalon Peninsula, and a weaker response in Conception Bay than in 2000. However, the model signal at Port Rexton, Trinity Bay, is weak in the 1999 case in comparison with the witness reports. The reason for the discrepancy is not clear at this time, although, as shown in Section 4.3, the model response is sensitive to the details of the storm track across the Banks.

The model results demonstrate the dependence of the dominant wave period comprising an event on the length scale of the atmospheric pressure forcing associated with the storm. An exception is Conception Bay where the model results are dominated by the resonant excitation of a seiche. Given a lack of observations, there is considerable uncertainty regarding the length scale of the forcing. However, the timing of the arrival of the event at the coast is much less dependent on this parameter. These conclusions are consistent with our expectations for non-rotating, non-dispersive gravity waves. On the other hand, the timing of the event, and its magnitude, depend strongly on the exact track taken by the storm over the Banks.

Predicting events, such as occurred along the east coast of Newfoundland in 1999 and 2000, is of obvious economic and social importance given the danger and damage that can occur. The success of the model simulations presented here demonstrates that a linear, barotropic model, such as we have used here, could be used as part of an operational prediction system. The most uncertain aspect of any prediction is likely to be in the determination of the exact track of the storm across the Banks, a factor our model results are quite sensitive to. It therefore makes sense that an operational prediction system should use a range of plausible storm tracks to access the risk of a significant event at the coast.

Acknowledgments

Travel and accommodation costs for the initial phases of this work were provided by the Environment Canada Learning Fund. We thank Dr. Hal Ritchie for arranging this funding and for helpful discussions. D.M. is also grateful for support from the Meteorological Service of Canada (MSC). J.S. and R.J.G. are supported by the Natural Sciences and Engineering Research Council of Canada (NSERC), MARTEC (a Halifax based company), and the Meteorological Service of Canada (MSC) through the NSERC/MARTEC/MSC Industrial Research Chair in "Regional Ocean Modeling and Prediction". Financial support for this work has also been received from the Canada Foundation for Innovation, and the Canadian Institute for Climate Studies. Meteorological data were supplied by the MSC and the Newfoundland Weather Centre, and tide gauge data by Fisheries and Oceans, Canada. The data report documenting the Acoustic Doppler Current Profiler data from St. John's harbour was kindly made available by Dr. Brad de Young of Memorial University, Newfoundland. Many eyewitnesses were extremely helpful, giving careful and honest reporting, and were generous with their time and with evidence such as photographs and video.

References

Abraham, G., Hurricane storm surge considered as a resonance phenomenon, *Proc. Conf. Coastal Eng.*, 7^{th}, The Hague, 585-602, 1961.

Bobanovic, J. and Thompson, K.R., The influence of local and remote winds on the synoptic sea level variability in the Gulf of Saint Lawrence, *Continental Shelf Research*, 21, 129-144, 2001.

Chapman, D.C., Numerical treatment of cross-shelf open boundaries in a barotropic coastal ocean model, *J. Phys. Oceanogr.*, 15, 1060-1075, 1985.

Churchill, D.D., Houston, S.H. and N.A. Bond, The Daytona Beach wave of 3-4 July 1992: A shallow-water gravity wave forced by a propagating squall line, *Bull. Am. Met. Soc.*, 76, 21-32, 1995.

de Young, B., Schillinger, D.J., Zedel, L. and J. Foley, *Physics and Physical Oceanography Technical Report 2000-1*, Department of Physics and Physical Oceanography, Memorial University of Newfoundland, St. John's, NF, Canada, 2000.

Donn, W.L., The Great Lakes surge of May 5 1952, *J. Geophys. Res.*,, 64, 191-198, 1959.

Ewing, M.F., F. Press and W.L. Donn, An explanation of the Lake Michigan surge of 26 June 1954, *Science*, 120, 684-686, 1954.

Geisler, J.E., Linear theory of the response of a two layer ocean to a moving hurricane, *Geophys. Fluid Dyn.*, 1, 249-272, 1970.

Gill, A.E., *Atmosphere-Ocean Dynamics*, Academic Press, San Diego, 662 pp., 1982.

Greatbatch, R.J., The response of the ocean to a moving storm: The non-linear dynamics. *J. Phys. Oceanogr.*, 13, 357-367, 1983.

Harris, H.D., Some problems involved in the study of storm surges, *National Hurricane Research Project*, Report 4, 1956.

Hughes, L.W., The prediction of surges in the southern basin of Lake Michigan. Part III: The operational basis for prediction. *Mon. Wea. Rev.*, 93, 292-296, 1965.

Irish, S.M., The prediction of surges in the southern basin of Lake Michigan. Part II: A case study of the surge of August 3 1960. *Mon. Wea. Rev.*, 93, 282-291, 1965.

Large, W.G., and S. Pond, Open ocean momentum flux measurements in moderate to strong winds, *J. Phys. Oceanogr.*, 11, 324-336, 1981.

Platzman, G.W., A numerical computation of the surge of 25 June 1954 on Lake Michigan, *Geophysica*, 6, 407-436, 1956.

Platzman, G.W., The prediction of surges in the southern basin of Lake Michigan. Part I: The dynamical basis for prediction, *Mon. Wea. Rev.*, 93, 275-281. 1965.

This manuscript was prepared with the AGU LaTeX macros v3.0.

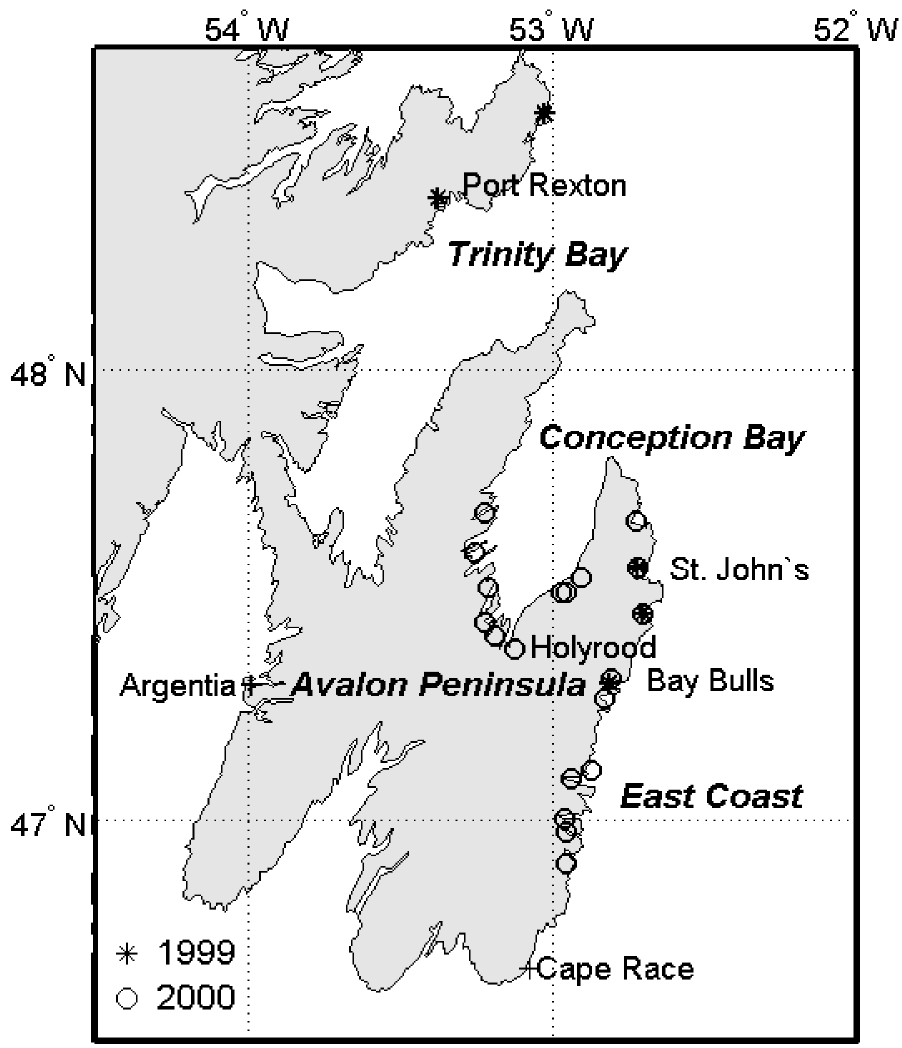

Figure 1: Southeastern Newfoundland showing locations with reports of wave events in 1999 (stars) and 2000 (circles).

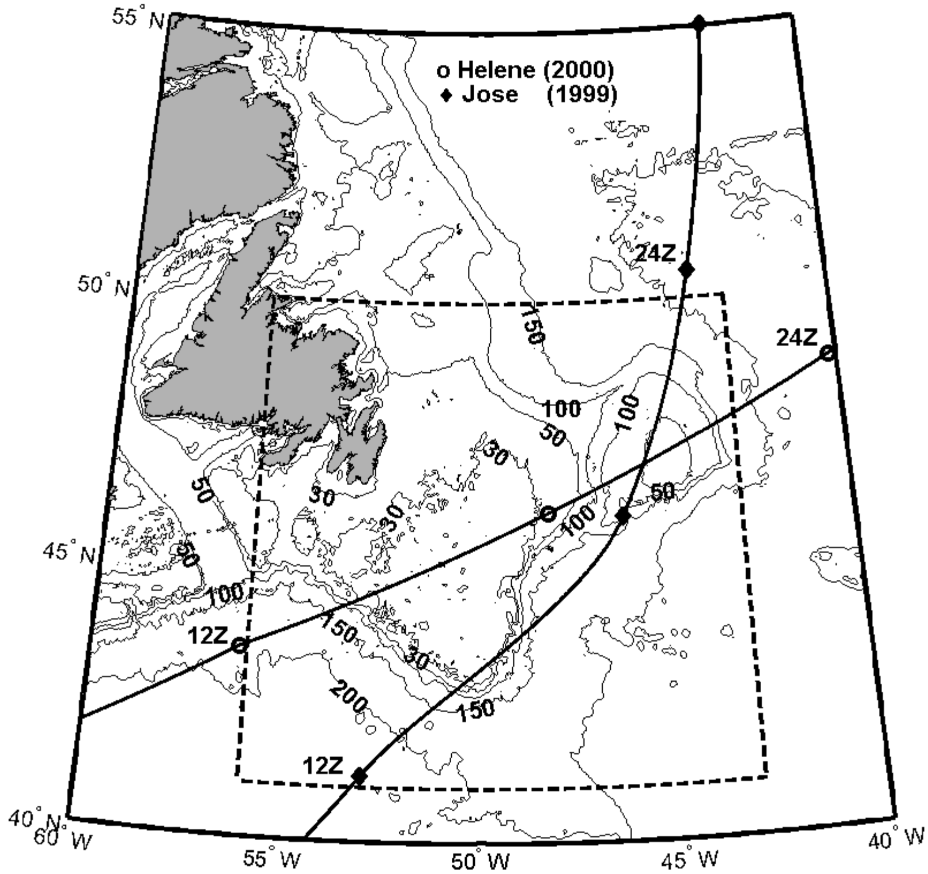

Figure 2: Map of study area. Newfoundland and Labrador are in grey. Six-hourly storm positions for Tropical Storms Helene and Jose are marked by circles and diamonds, respectively (courtesy of Newfoundland Weather Centre). The contours are shallow water gravity wave speed in ms^{-1}, and are related to water depth, H, by $c = \sqrt{gH}$. The boundary of the model domain is shown by the dashed box.

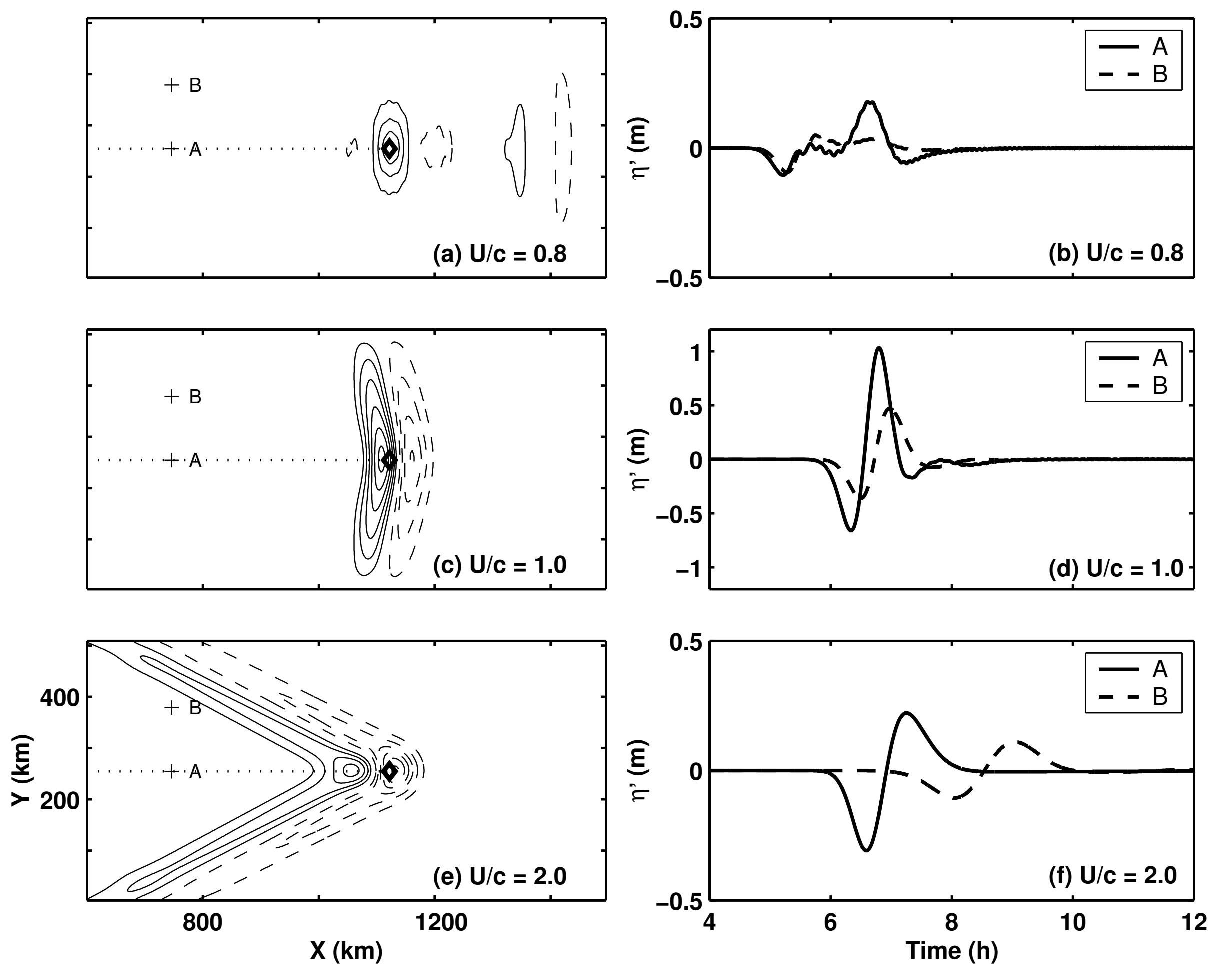

Figure 3: Adjusted sea level as a function of U/c. In (a), (c), and (e) the storm centre is marked by a diamond, the storm track is a dotted line, and the crosses labeled A and B mark the positions where time series of adjusted sea level are plotted in (b), (d), and (f), respectively. Positive contours are solid, negative contours are dashed, and the contour interval is 0.2 m in (c) and 0.05 m in both (a) and (e). The zero contour is not shown. Note that the contour plots only show part of the model domain, and the use of different scales in (b), (d) and (f).

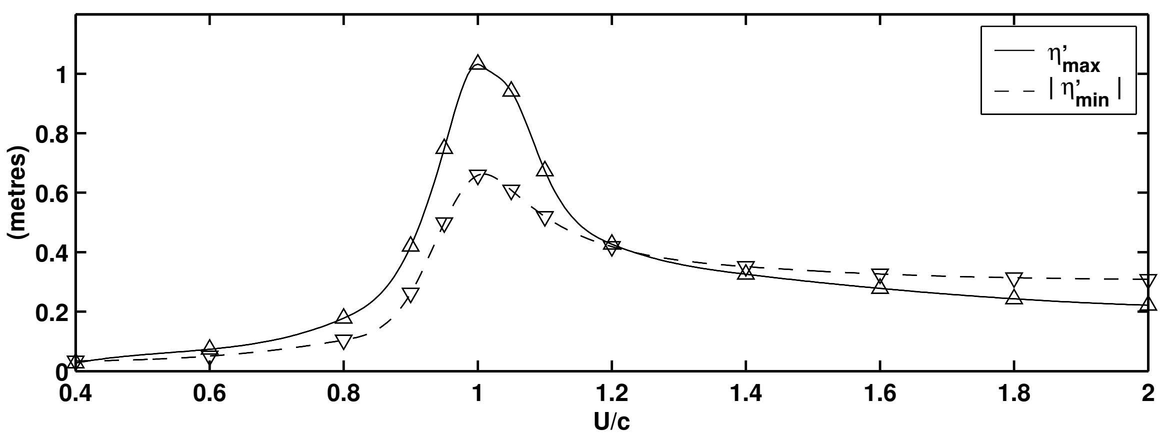

Figure 4: Maximum rise (solid line) and fall (dashed line) of adjusted sea level as a function of U/c at a point along the storm track.

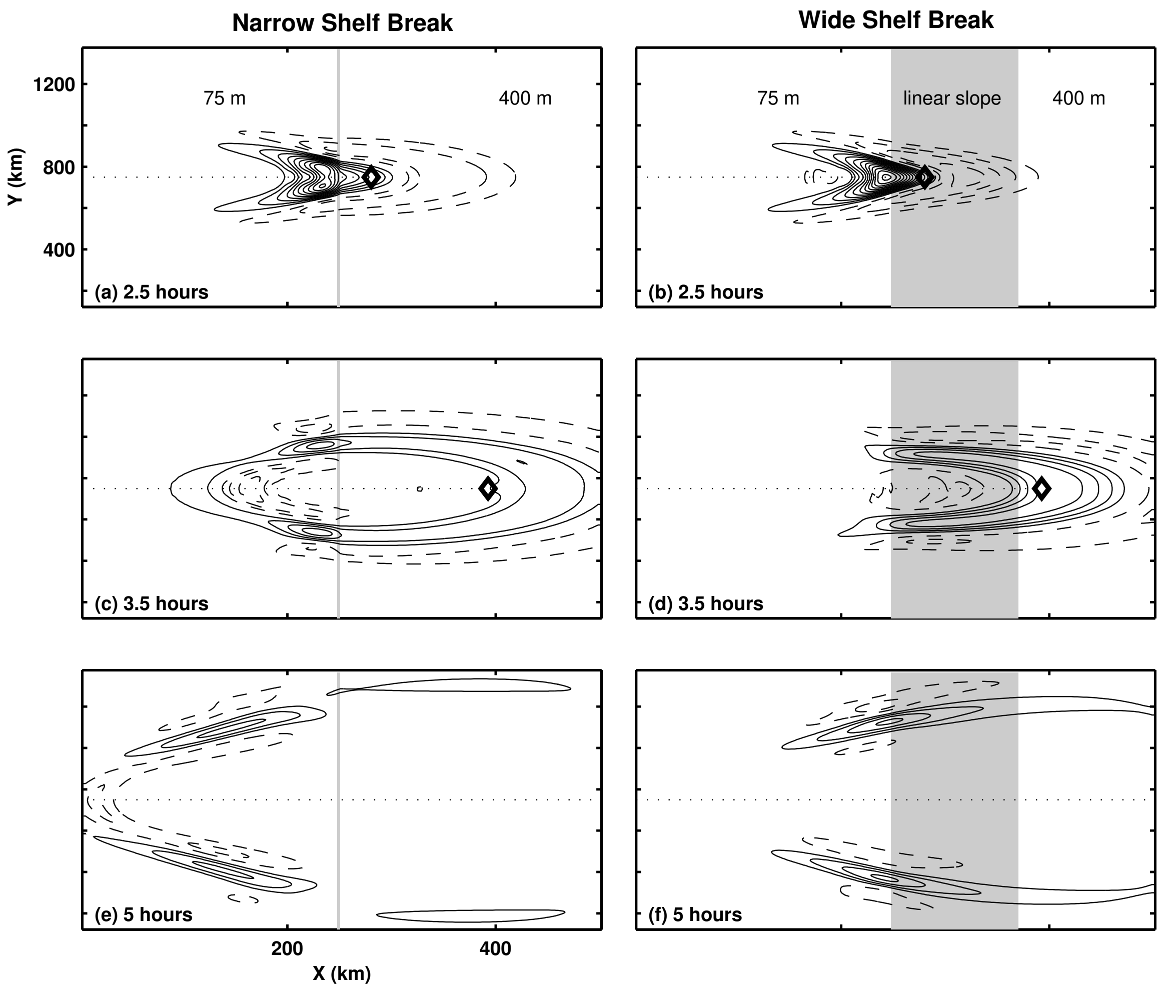

Figure 5: Transition of storm from shallow water to deep water. In every case the storm moves from shallow (75 m or $U/c = 0.8$) to deep water (400 m or $U/c = 2.0$) across a shelf break. The shelf break is shaded in grey and starts at 250 km east of the western boundary; in the narrow shelf break case it is 3 km (i.e. one grid point) wide, while in the wide shelf break case it is 120 km wide. (a), (c), and (e) are successive images for the narrow shelf break case, while (b), (d), and (f) are the corresponding images for the wide shelf break case. The storm centre is marked by a diamond, and the storm track by a dotted line. Contours are in 0.05 m increments, with solid contours positive and dashed negative. The zero contour is not shown.

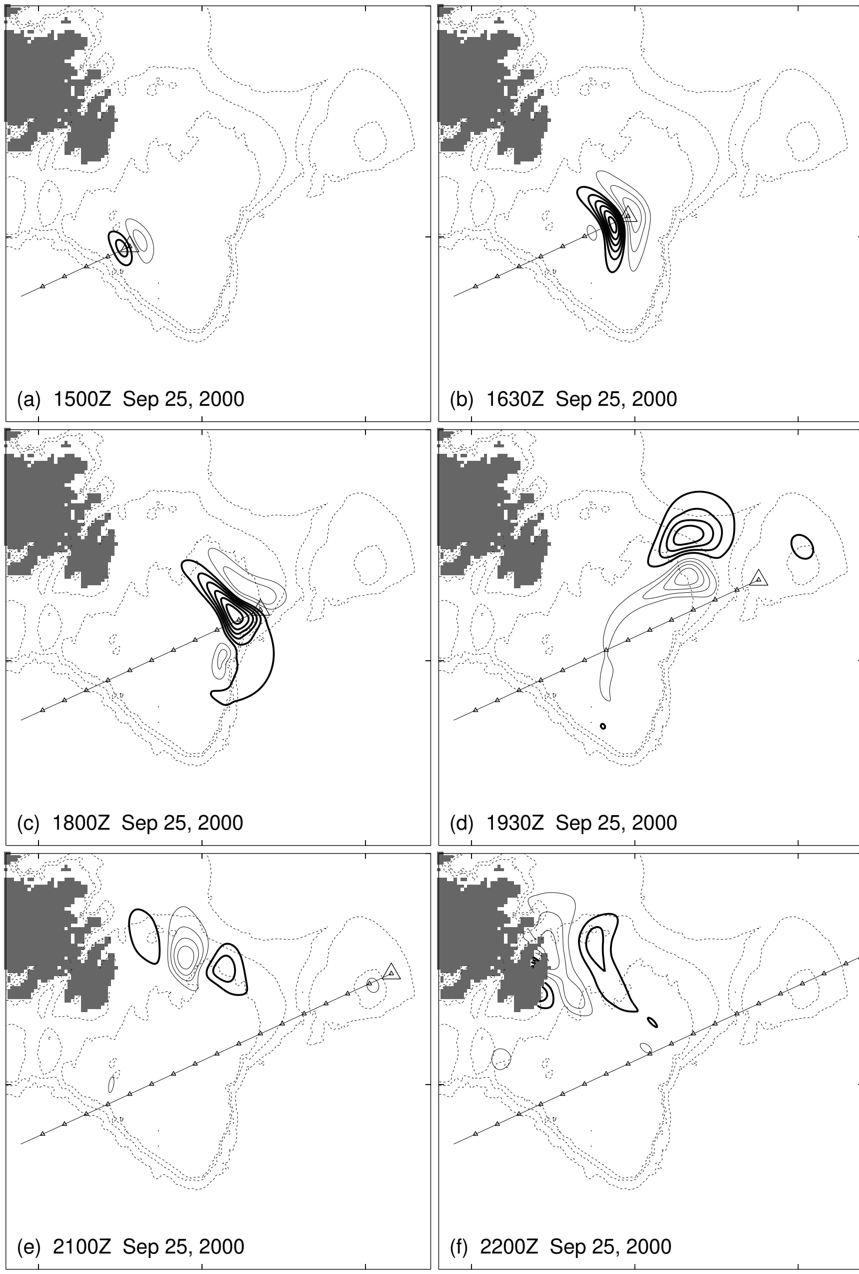

Figure 6: Simulation of ocean response to Tropical Storm Helene on September 25, 2000. Contours are of adjusted sea level, with thick contours positive and thin contours negative. The contour interval is 0.1 m, and the zero contour is not shown. The storm track is marked every 30 minutes with black triangles, and the current storm position is marked with a large triangle. The dotted lines are bottom contours at 100, 400, and 1000 metres.

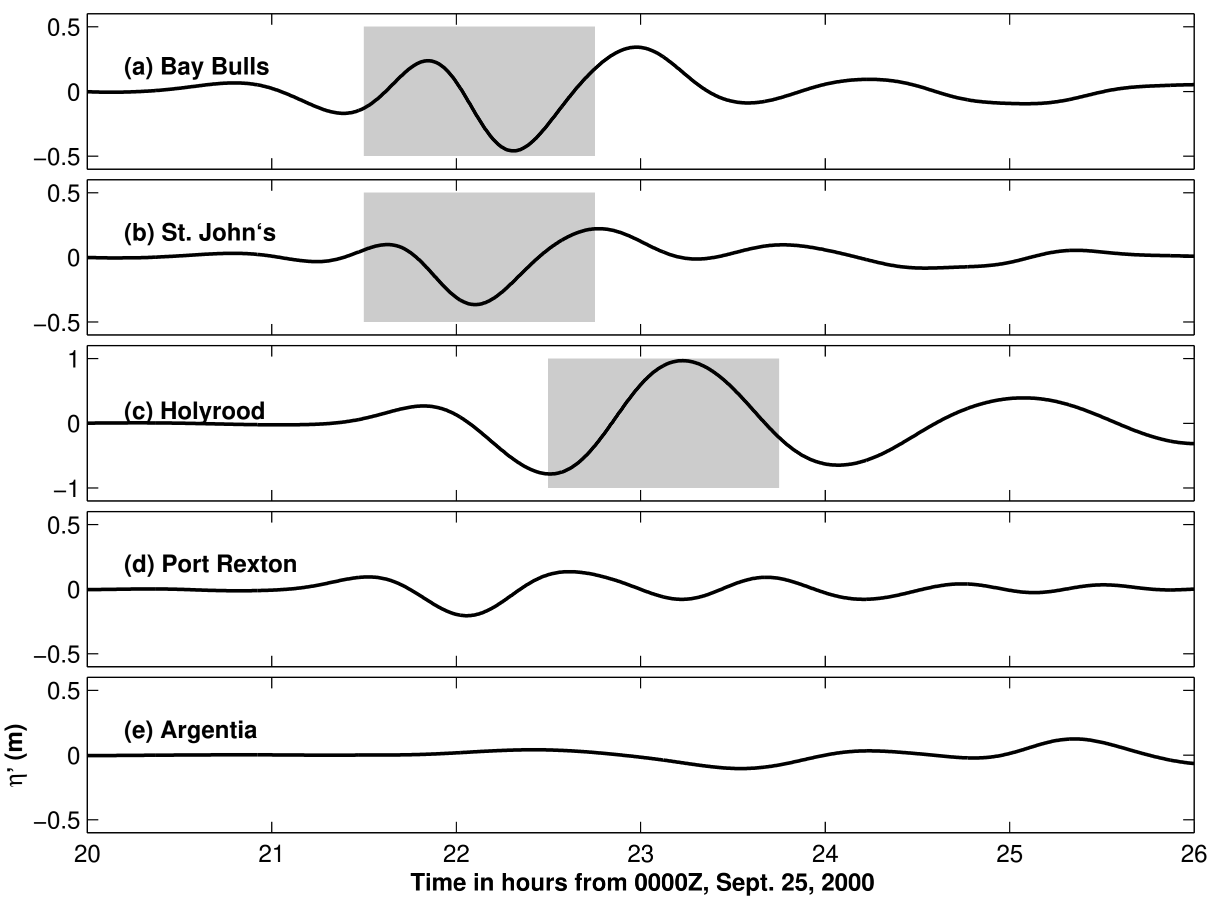

Figure 7: Time series of the model-computed adjusted sea level response to Tropical Storm Helene at five locations in southeastern Newfoundland. Shaded boxes indicate approximate time frame for the actual event from witness reports and other data for each location. The units are meters. Note the use of a different scale at Holyrood.

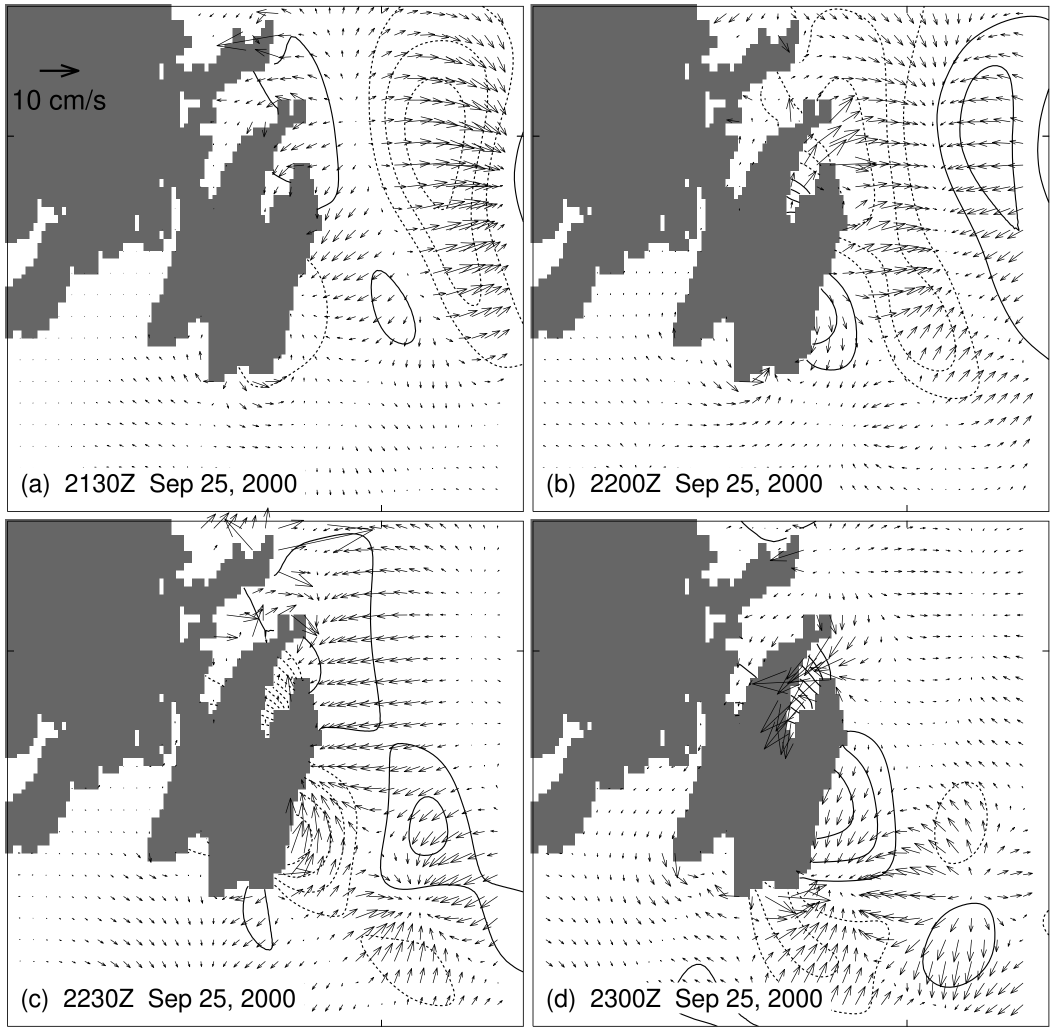

Figure 8: Model-computed adjusted sea level and barotropic currents in response to Tropical Storm Helene. The contour interval is 0.1 m, with solid contours positive and dotted contours negative. The zero contour is not shown. Current vectors are plotted every third grid point in both the zonal and meridional directions.

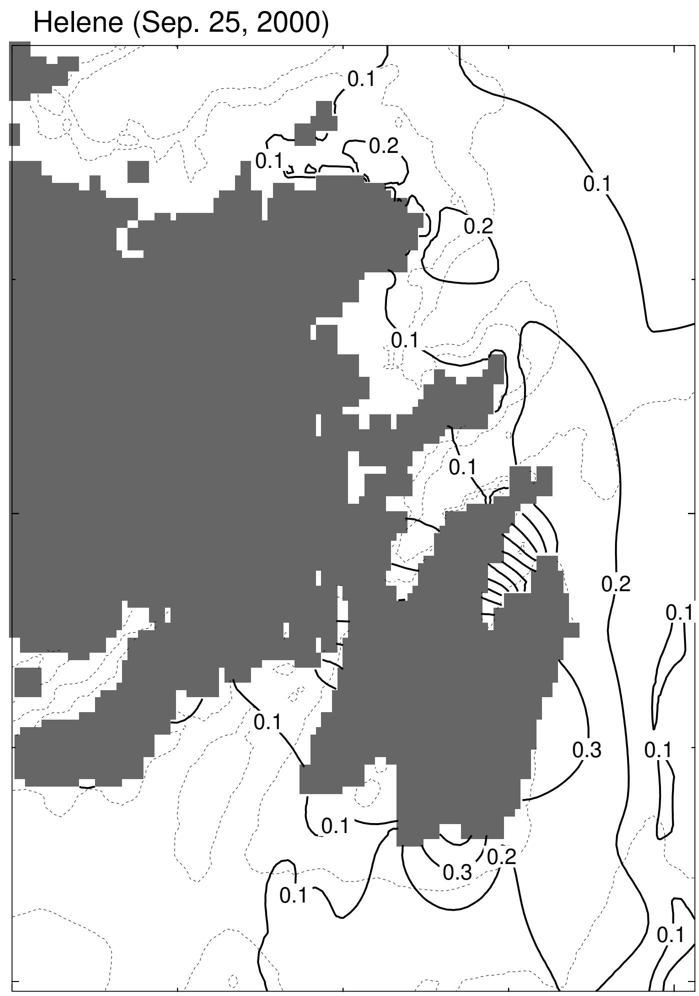

Figure 9: Maximum set-up in adjusted sea level near southeastern Newfoundland in the standard Tropical Storm Helene model run. The contour interval is 0.1 m.

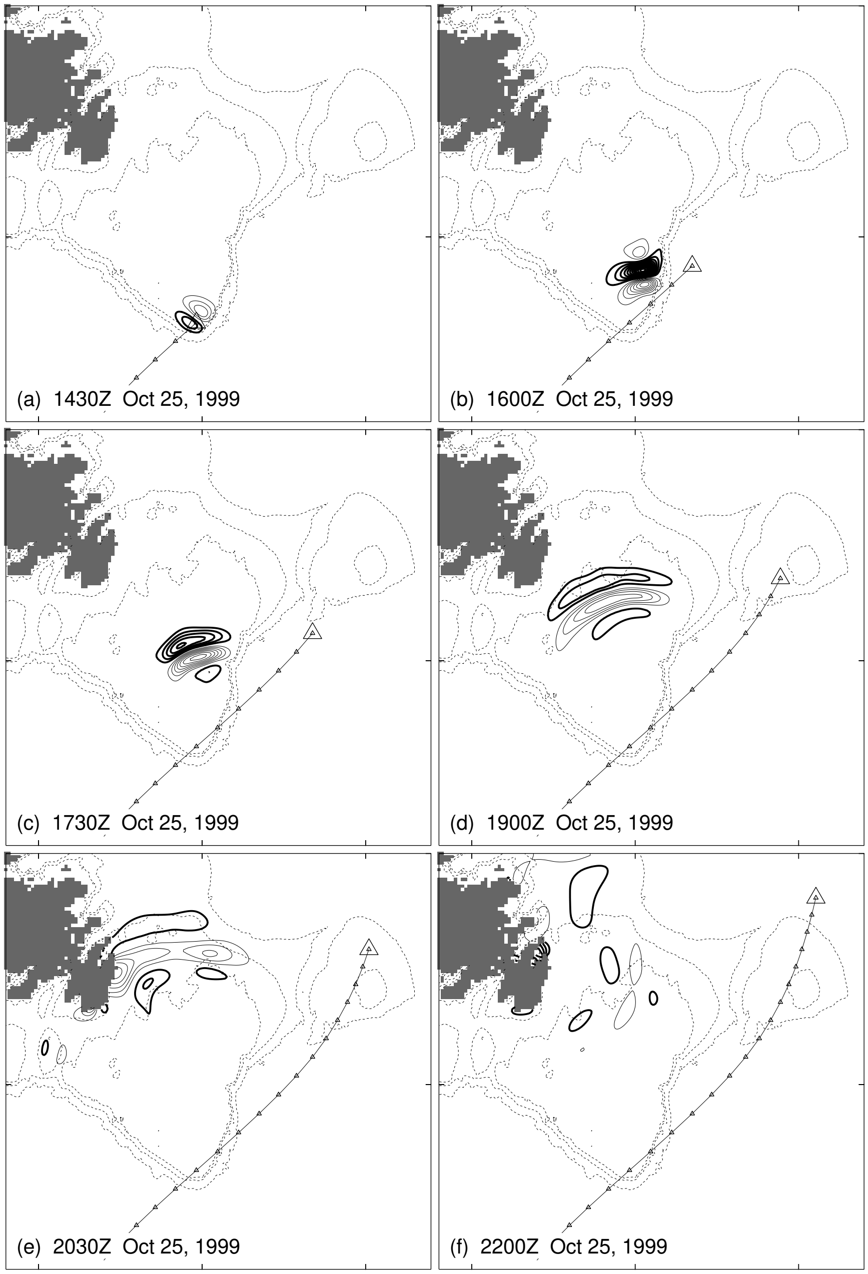

Figure 10: Simulation of the ocean response to Tropical Storm Jose on October 25, 1999. Contours are of adjusted sea level, with thick contours positive and thin contours negative. The contour interval is 0.05 m and the zero contour is not shown. The storm track is marked every 30 minutes with black triangles, and the current storm position is marked with a large triangle. The dotted lines are bottom contours at 100, 400, and 1000 metres.

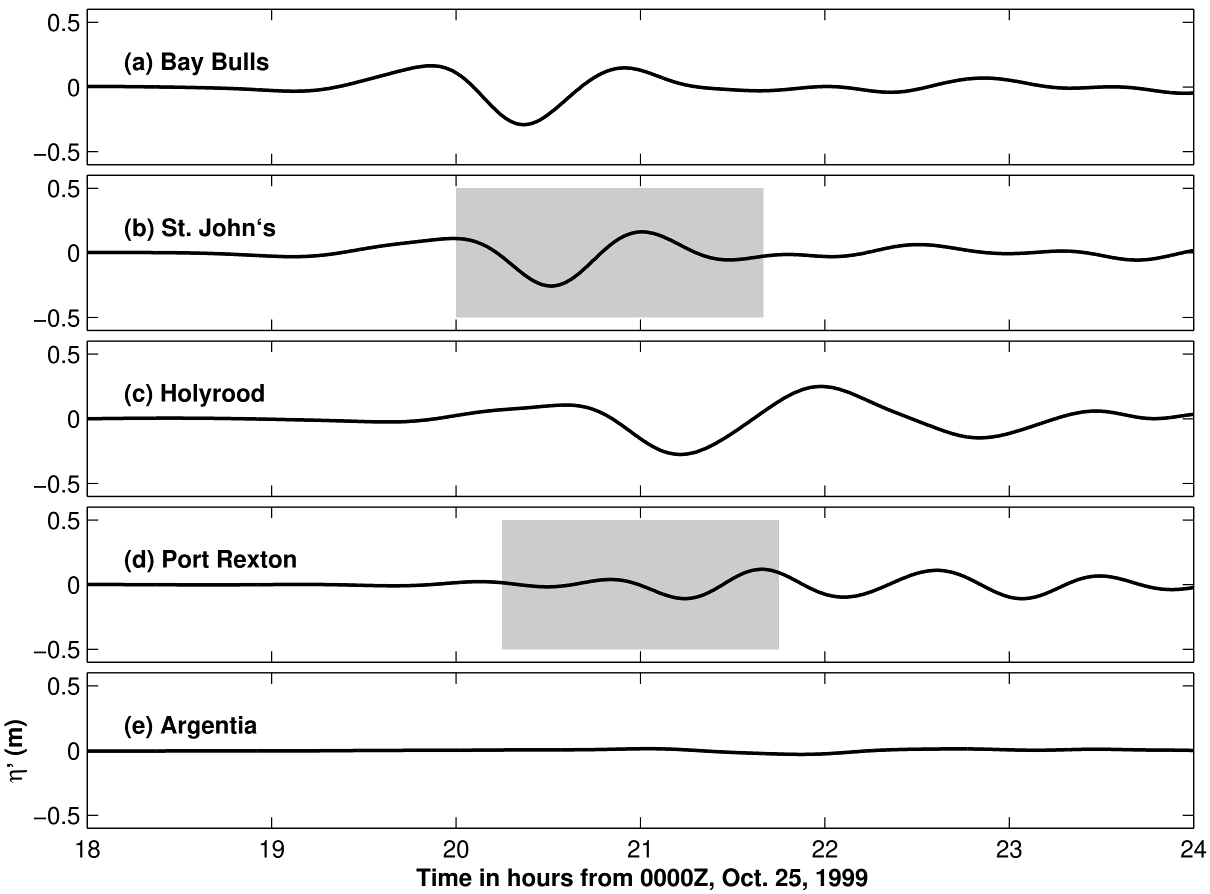

Figure 11: Time series of the model-computed response in adjusted sea level to Tropical Storm Jose at five locations in southeastern Newfoundland. Shaded boxes indicate the approximate time frame for the actual event from witness reports or other data from each area. The units are meters.

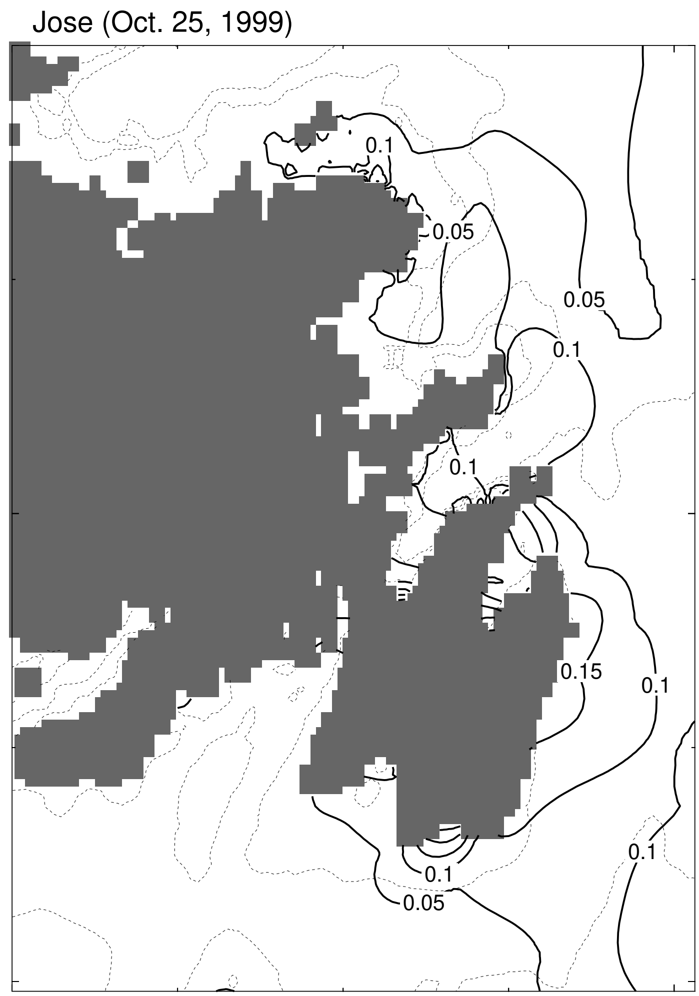

Figure 12: As Figure 9 but for Tropical Storm Jose. The contour interval is 0.05 m.

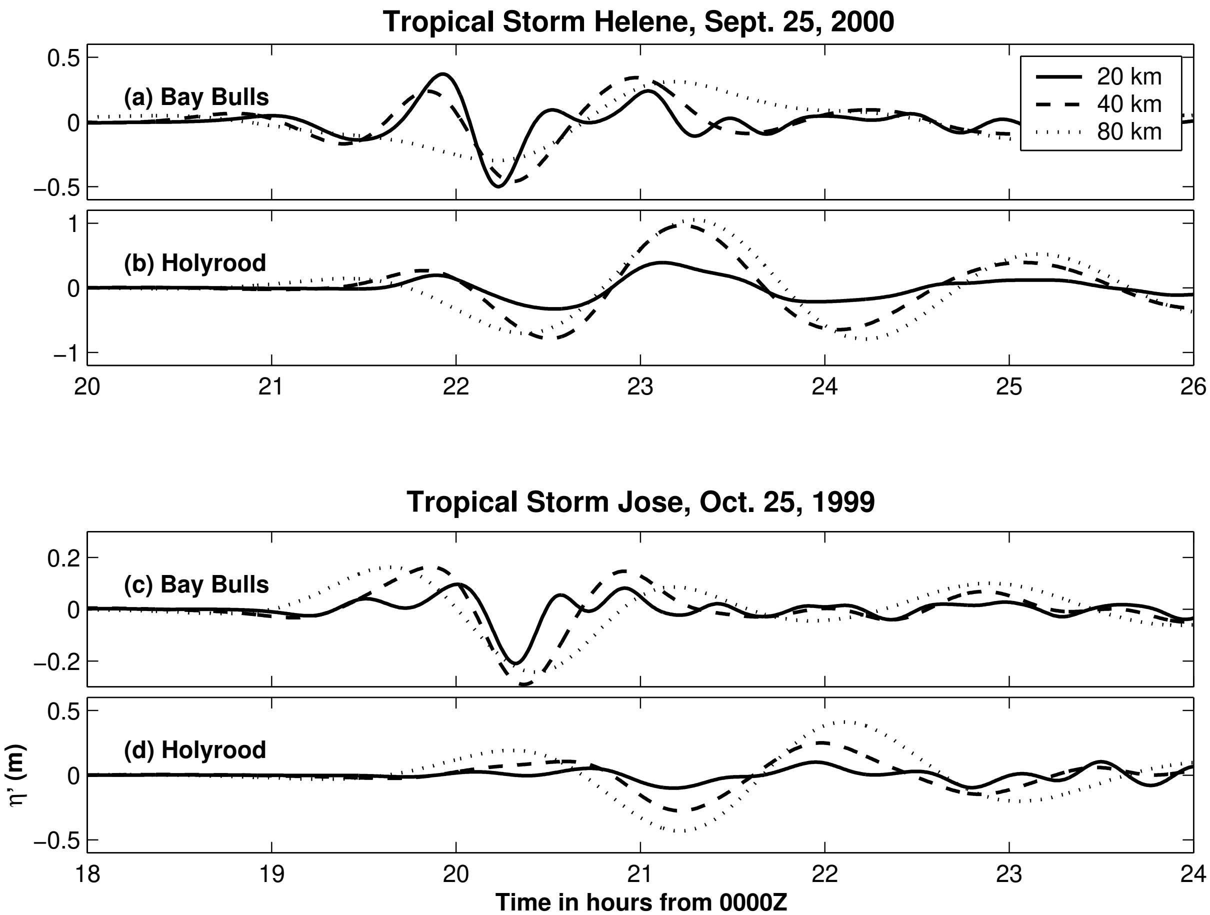

Figure 13: Sensitivity of the near shore model response to the length scale used for the forcing (see text for details). Bay Bulls is representative of the East Coast and Holyrood is representative of southern Conception Bay. The time series are of adjusted sea level in metres. Note the lower amplitudes in (c) and (d) for the Tropical Storm Jose simulation, and the use of different scales.

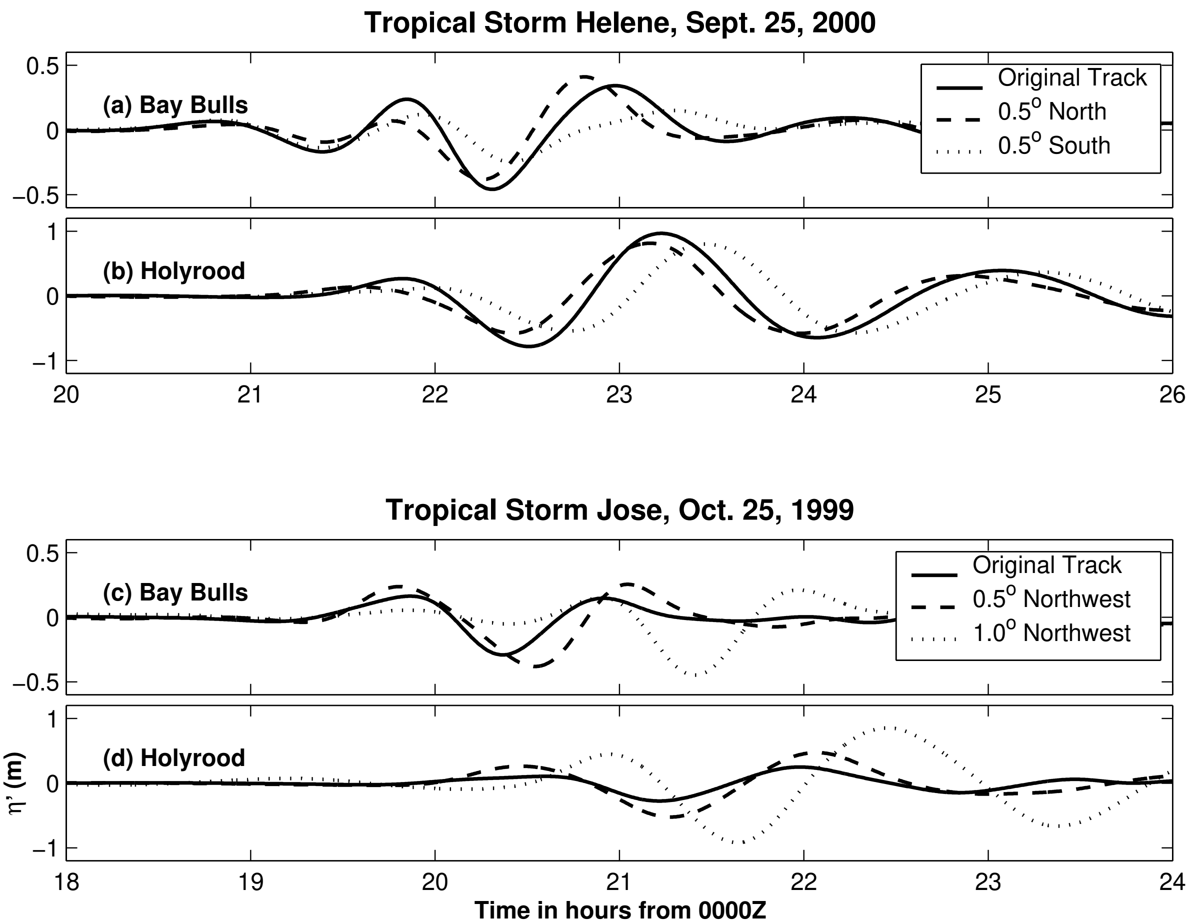

Figure 14: Sensitivity of the near shore ocean response to perturbations in storm track, for both Tropical Storms Helene and Jose. The time series are of adjusted sea level in metres.